Holzforschung, Vol. 66, pp. 993–1000, 2012 • Copyright © by Walter de Gruyter • Berlin • Boston. DOI 10.1515/hf-2011-0136

# Nano- and microstructures in stretched and non-stretched blend gels of cellulose and hemicelluloses

**Johannes P. Roubroeks[a] and Tetsuo Kondo***

Graduate School of Bioresource and Bioenvironmental Sciences, Kyushu University, 6-10-1 Hakozaki, Higashi-ku, Fukuoka 812-8581, Japan

*Corresponding author.
Graduate School of Bioresource and Bioenvironmental Sciences
Kyushu University, 6-10-1 Hakozaki, Higashi-ku, Fukuoka 812-8581, Japan
Phone: +81-(0)92-642-2997
Fax: +81-(0)92-642-2997
E-mail: tekondo@agr.kyushu-u.ac.jp

## Abstract

Molecular interactions between cellulose and hemicelluloses, such as xyloglucan and xylan, play an important role in the formation of ordered layers in the cell wall of higher plants. This study attempts to characterize an ordered state of a matrix consisting of cellulose and hemicellulose induced by stretching never-dried binary blended films. In non-stretched films, the xylan component easily adapted into the semicrystalline state, while the xyloglucan component remained amorphous. Once both blended films were stretched, each component tended to be close enough to the adherent macromolecule, and the interaction resulted in typical morphological orders at the nano- and microscale levels. These studies could be useful in constructing new bio-derived materials, as well as understanding the molecular interactions between the polymers.

**Keywords:** cellulose; hemicellulloses; molecular interactions; nano/microstructure; ordered layer.

## Introduction

The plant cell wall is a highly organized composite material consisting of various polysaccharides, proteins, and lignin (Carpita and McCann 2000) with a special supramolecular architecture (Salmén and Burgert 2009; Stevanic and Salmén 2009). The most abundant plant polysaccharide, cellulose, accounts for 15–30% of the dry mass of the primary and ca. 43% of secondary cell walls. Upon deposition of newly biosynthesized polymeric components in the primary cell wall, it has been shown that the cellulose microfibrils are well aligned, whereas the morphology and crystalline state change through the developing stage in the secondary wall (Abe et al. 1995, 1997). The regulatory role of the hemicellulose during secondary wall deposition has been frequently reported (Vian et al. 1986; Neville 1988; Atalla et al. 1993) as well as their state of interaction with other polymers (Uhlin et al. 1995; Iwata et al. 1998). The interdependent regulatory organization between cellulose nanofibers and hemicellulose molecules remains a point of debate, but the interfacial interaction between them may be still strongly affected by the similarity of the primary structure of the involved macromolecules.

In the primary cell wall, the cellulosic scaffold is interlocked by xyloglucan. Xyloglucan consists of linear chains of (1→4)-β-D-glucan with numerous α-D-xylose units linked at regular positions to the O-6 of the anhydroglucose units. Some xylosyl residues are further substituted at O-2 by β-D-Gal*p* residues, and some of the galactose residues may be substituted at O-2 by α-D-Fuc*p* (Hayashi and MacLachlan 1984; Hayashi 1989). Models of the architecture of dicotyledon primary walls commonly assume that xyloglucans are adsorbed to coat the cellulose microfibrils (McCann et al. 1990; Whitney et al. 1995; Cosgrove 2001). The cellulose becomes less crystalline (*p*-crystalline), and also, the Iα/Iβ crystallite ratio is decreasing without any significant alteration in the fibril diameter (Whitney et al. 1995). NMR data (Whitney et al. 1995) and molecular dynamics simulations (Levy et al. 1991; Kroon-Batenburg et al. 1993; Hanus and Mazeau 2006) on xyloglucan/cellulose composites provide evidence for a transition of the "twisted" to the "flat" conformation upon binding. In this way, the backbone structure of xyloglucan would resemble the cellulose structure to a large extent, which may enhance the close interaction between cellulose and xyloglucan (Hayashi et al. 1994; Finkenstadt et al. 1995), possibly in a partly ordered fashion rather than in an amorphous state (Bootten et al. 2009).

In the secondary walls of hardwoods, glucuronoxylan is the main polymer constituent of the hemicelluloses moiety (20–35%). It has been suggested that this polymer is involved in establishing the orientation of the microfibrillar cellulose during cell wall formation (Neville 1988; Reis et al. 1994). Glucuronoxylans are composed of a linear backbone of (1→4)-β-linked xylopyranosyl residues, substituted with short mobile side groups, which are α-glucuronic acid (or its 4-O-methyl ester) mainly at O-2. The distribution of these side groups (one per 10 xylose residues on average) (Jacobs et al. 2001) determines the solubility of the polymer and also affects the capability of interaction with other polymers (Reis et al. 1994; Ebringerová and Heinze 1999).

The interfacial interactions have been recognized at an early stage to be responsible for biological, physical, and mechanical properties of the plant cell wall. Various techniques proved

[a]Present address: Novozymes Biopharma A/S, Krogshoejvej 36, 2880 Bagsvaerd, Denmark.

to be useful to investigate the complex interactions (Whitney et al. 1995; Whitney et al. 1998; Åkerholm and Salmén 2001; Cosgrove 2001). However, the importance of molecular miscibility has not yet been addressed satisfactorily, though the molecular miscibility in polymer blends is a fundamental requirement to alter the polymer properties. To fill this gap, this paper focuses on cellulose-hemicellulose blends in terms of molecular miscibility. After molecular mixing, the focus is on the change of the miscibility by stretching which induces orientation. The expectation is that these results could contribute to a better understanding of the matrix structure of the plant cell wall.

## Materials and methods

### Materials

Bleached cotton linters, with a degree of polymerization (DP) of 1300, was one of the starting materials. By means of a water-methanol solvent exchange technique, the cellulose (final conc. 1%) was completely dissolved in dimethyl acetamide (DMAc)/LiCl solvent system (Kondo et al. 2001). Beechwood xylan (DP 42) was provided by Lenzing AG (Lenzing, Austria) and was dissolved in a similar solvent system (final conc. 2.2%). The xylan is composed of 95% xylose and contains only between 1% and 2% of glucuronic acid. This renders the primary structure very similar to cellulose. Xyloglucan (Tamarind seed Mw ~200 kDa) was purchased from Megazyme (Bray, Ireland) and dissolved also in DMAc/LiCl system (conc. 1%). Blends with cellulose were prepared from the individual solutions, and compositions of the blends varied from 0% to 90% (w/w) for xylan and from 0% to 50% (w/w) for xyloglucan, respectively.

### Sample preparation

A time span of 10 days was required for complete mixing before the samples were poured into flat-bottomed Petri dishes. Then, coagulation of the solution occurred in 3 days under saturated water vapor. The precipitates were extensively washed and kept in the refrigerator. 1) Non-stretched films: The gel-like films were dried at room temperature between objective slides. 2) Stretched films: The method was followed as previously described for nematic ordered cellulose (NOC) (Kondo et al. 2001).

### Wide-angle X-ray diffraction (WAXD)

WAXD photographs were taken on a flat film using Ni filtered CuKα radiation produced by a RINT-2500 HF X-ray generator (Rigaku Co. Ltd, Tokyo, Japan) at 40 kV and 40mA. The WAXD intensity curves with a scanning speed of 0.5° $min^{-1}$ were measured by a transmission method in a scintillation counter at 40 kV and 200 mA through the angular range 2θ for both the equatorial and meridional scans to the drawing direction; 2θ=5–35° and 10–60°, respectively.

### Dynamic force microscopy (DFM)

DFM images of the stretched cellulose-xylan and cellulose-xyloglucan blend films were acquired on a SPA-300HV (Seiko Instruments Inc., Tokyo, Japan). DFM measurements were performed at room temperature, being controlled in tapping mode. The cantilever for DFM was SI-DF20 (SII, silicone made) with a spring constant of 15 N $m^{-1}$. The scan frequency was 0.5–2.0 Hz depending on the scale, and the observed areas varied from 5×5 $\mu m^2$ to 1×1 $\mu m^2$. The surface roughness was assessed by topographical software (Seiko Instruments Inc., Tokyo, Japan).

### Light microscopy

Sample preparation was as follows: 1 ml of solution was evenly distributed in a small flat-bottomed Petri dish. The Petri dishes were then placed into a convection oven at 50°C for a 10-day period, for faster solvent evaporation. Distilled water was added, and after washing thoroughly (it is required to remove all the LiCl crystals), the gel-like film was transferred to a cover glass before it was returned to the oven for another week. Light microscopic images were acquired with a 40×/0.75 PH 2 HCX PL Fluotar objective lens (Leica, Microsystems, Tokyo, Japan) coupled with an ×1.25 optivar lens by means of a Leica DMRE microscope with a C5810 color chilled 3CCD camera (Hamamatsu Photonics Co. Ltd, Shizuoka, Japan). Digitized frames were captured, saved, and processed with Image PRO PLUS 4.1 software (Media Cybernetics, Bethesda, MD, USA).

### Microscopic FTIR

Samples examined by Micro 20 microsampling FTIR spectrophotometer (JASCO Co. Ltd, Tokyo, Japan) were prepared in a similar fashion as described above. A glass slide was covered with solution to be slowly submerged into a water bath. Then, the solution was coagulated to provide the gel. For measurements, it was put on a TEM grid, and the measurement area was 12 μm×12 μm.

## Results and discussion

The use of water vapor is critical in our approach for the assembly of polymer components and to establish the interfacial interaction. Therefore, to obtain blended films of cellulose and hemicelluloses, a previously developed method for the preparation of NOC was employed (Kondo et al. 2001). Ultimately, this could provide a gel-like film. After thorough washing with water, the water-swollen films consisting of only cellulose were always completely transparent. Previously, it was determined that the gels were composed of approx. 93% water and 7% cellulose (Kondo et al. 2001).

### Non-stretched films of cellulose-hemicellulose blends

Like the water-swollen cellulose gels, the non-stretched cellulose-xyloglucan gels were completely transparent. The condition was maintained when the films were completely dried. This indicated that mixing of the blend and its coagulation under saturated water vapor did not initiate a co-crystallization or phase separation. In fact, no contribution due to crystallinity could be observed in WAX diffractograms. Accordingly, both polymers were compatible to coexist in an amorphous state (Figure 1a). On the contrary, the precipitated gels containing xylan were changing from transparency to completely white opacity depending on the composition. At higher concentrations of xylan, the blended gel turned white and remained non-transparent after complete drying. Cellulose-xylan composites showed

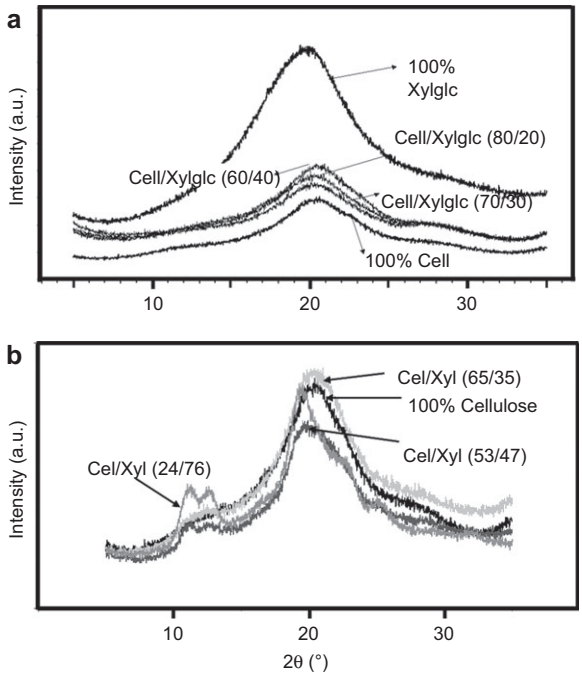


**Figure 1** Equatorial diffraction intensity patterns of (a) non-stretched dried cellulose-xyloglucan blend films and (b) non-stretched dried cellulose-xylan blend films. Compositions as %.

a tendency for self-assembly of xylan at higher concentrations in the blends with cellulose, as indicated by the WAXD pattern of Figure 1b. Namely, the contribution of a semicrystalline state of the xylan could be neglected at xylan concentrations lower than 65/35% of cellulose-xylan, still in favor of the low-crystalline (13%) NOC state (Kondo et al. 2001). Higher xylan concentrations favor self-assembly forming a semicrystalline state. At a composition of 53/47% of cellulose-xylan (Figure 1b), diffraction peaks at 11.4° ($d$=0.78 nm) and 12.9° ($d$=0.69 nm) appeared. Moreover, the main diffraction peak at 20° started to shift toward higher $d$ values, and the peak became more distorted. Increasing the concentration of xylan resulted in a diffraction intensity pattern that is almost identical to the hydrated state of 4-O-methyl glucuronoxylan from white birch (Marchessault and Settineri 1964). The change of X-ray diffraction indicated that phase separation, due to xylan self-assembly, between cellulose and xylan occurred at xylan concentrations higher than 65/35% cellulose-xylan.

The phase separation due to the self-assembly of xylan in non-stretched films in the presence of cellulose was also investigated by light microscopy. To this purpose, the individual blended cast films were carefully prepared at concentrations below 50% of cellulose. In the blended cast film of 24/76% of cellulose-xylan, organized spherulitic structures were clearly observed under a cross-Nicols of a polarized microscope (Figure 2a). They could only be observed at higher xylan compositions than 50% in the presence of cellulose. This appearance corresponds to the semicrystalline state of xylan as shown in Figure 1b (24/76%). The size of the spherulite structures was around 38 μm in average. The microscopic FTIR measurements, focusing at the center of the round shape (Figure 2b), revealed that it resembles the typical spectrum of polysaccharides including cellulose or xylan (Figure 2c). As cellulose is covering across the entire film area, no significant difference could be observed. Because of a lacking of -$CH_2$- rocking vibration in the range of 700–750 $cm^{-1}$ (inset of Figure 2c), cellulose in the blend is

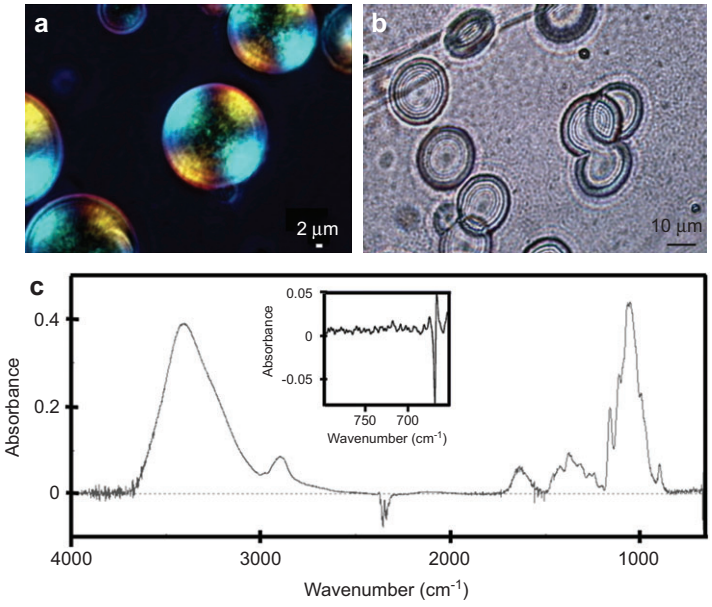


**Figure 2** (a) Observation of possible xylan crystals under crossed-Nicols of a polarized microscope. 24/76% cellulose-xylan. Band spacing is about 1.1 μm. (b) Microscopic image of the cast gel focused by IR irradiation and single crystal. (c) FT-IR spectrum. Inset shows a specific area of -$CH_2$- rocking vibration in the entire spectrum.

not an original native crystalline form (Sugiyama et al. 1991; Kataoka and Kondo 1999). Therefore, the observed crystalline spheres were derived from xylan in a semicrystalline state, which was phase separated from the surrounding cellulose matrix in the film. The structure may consist of many ordered xylan crystals, as the spherulites consist of a large number of crystals radiating in all directions from one point (Mandelkern 1964).

The above results displayed that the assembly in both cellulose-xyloglucan and cellulose-xylan blends were completely different in the mixing behavior. Blends of cellulose and xylan were strongly influenced by the concentration of xylan. In particular, the phase separation due to self-assembly of xylan molecules occurred out of the surrounding matrix at concentrations higher than 35%. Blends of cellulose-xyloglucan are fully compatible to coexist and could therefore engage a tight interaction, despite the presence of short substituents on the xyloglucan chain.

### Stretched films of cellulose-hemicellulose blends

Native plant cell walls appear to occur largely as an ordered structure possibly due to geometrical constraints or physiological stress. Thus, it was required to investigate the cellulose-hemicellulose blends in an ordered state. NOC films, namely, uniaxially stretching of the water-swollen cellulose film, provided highly ordered, parallel-aligned molecular glucan chains in a non-crystalline state (Kondo et al. 2001). This state did not change after drying to a solid-state film. In a previous paper, WAXD patterns in conjunction with the intensity curves in both the equatorial and meridional directions for the NOC film exhibited the presence of a unique state, the nematic ordered state (Kondo et al. 2001).

After stretching the cellulose-xyloglucan blended films with various compositions, the WAXD intensity curves at an equatorial direction are virtually identical to the equatorial diffraction pattern of NOC (Figure 3a). No significant change in fiber X-ray diffraction patterns for the blended films was observed when compared with that for NOC (insets in Figure 3a). Therefore, no influence of addition of xyloglucan can be observed on the order. In particular, the meridional diffraction patterns (Figure 3b) showed a virtual similarity to that for NOC. It is therefore likely that cellulose and xyloglucan were mixed in a close interaction with each other. In addition, the interacting cellulosic and non-cellulosic molecular chains were capable of being aligned to give the order like NOC. It has been shown by NMR (Whitney et al. 1995) that the chemical shift of glucosyl C1 of xyloglucan is essentially identical to that of cellulose as a common conformation.

The WAXD intensity curves for a set of stretched cellulose-xylan blends with a varying composition are presented in Figure 4. The equatorial diffraction patterns for all cellulose-xylan compositions (Figure 4a) showed a very similar X-ray diffraction pattern to the NOC. However, the differences became very clear in the fiber patterns (insets in Figure 4). Here, a high order could be recognized in the blend of 85/15% of cellulose-xylan, while no clear arcs, indicating a non-ordered state, are obtained at a composition of 24/76% of cellulose-xylan. The meridional scan (Figure 4b) was employed to analyze the order along the fiber direction of the stretched sample. In general, meridional intensities are affected by the disorder of the neighboring chains, which are symmetrical with the chain axis (Kondo et al. 2001). The reflections thus found indicate that

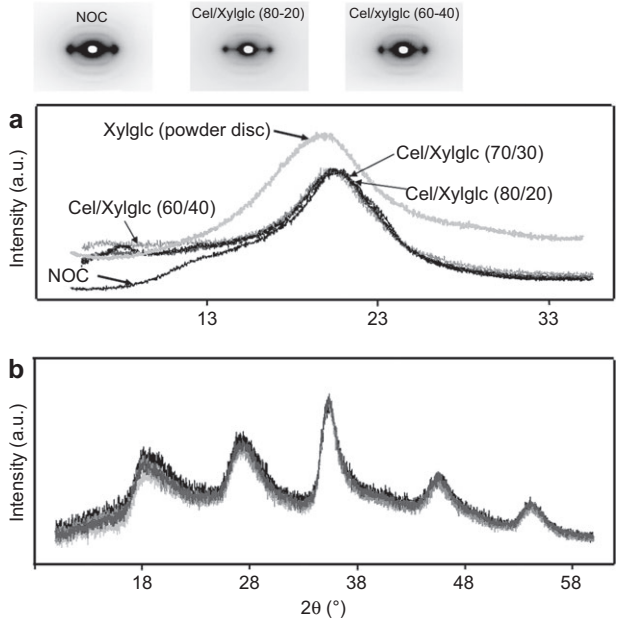


**Figure 3** (a) Equatorial and (b) meridional X-ray diffraction patterns of stretched cellulose-xyloglucan blended films. Insets show the fiber X-ray patterns of stretched cellulose-xyloglucan blended films in comparison to NOC.

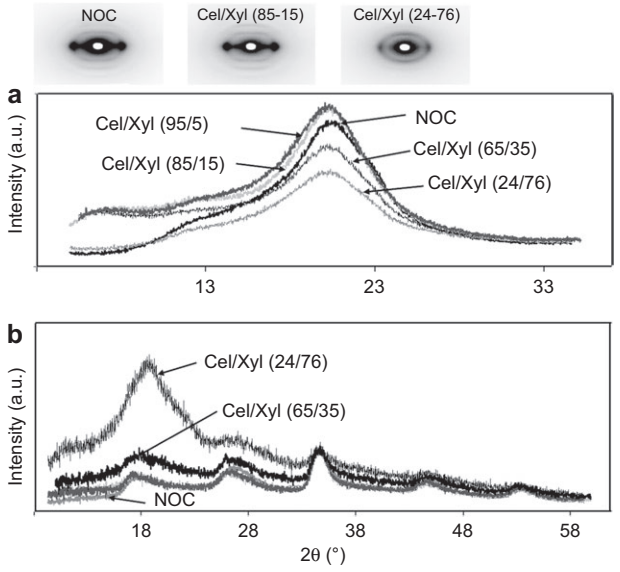


**Figure 4** (a) Equatorial and (b) meridional X-ray diffraction patterns of stretched cellulose-xylan blended films. Insets show the fiber diffraction patterns of stretched cellulose-xylan blended films in comparison to NOC.

a certain disorder occurred in the structure of the stretched cellulose-xylan blends. At xylan concentrations below 30% (Figure 4b), the meridional scans were very similar, indicating compatibility between the two polymers possibly due to molecular interaction. However, an increase of the xylan composition in the blends resulted in a deviation from the ability of being aligned and hence facilitates the loss of its nematic order. The increasing meridional diffraction of the (002)- and (003) plane, if a crystalline lattice was assumed, revealed the formation of ordered, semicrystalline xylan domains. At a composition of 24/76% cellulose-xylan, the predominant reflection in the meridional scans represented a xylan domain, in which the nematic order might be greatly reduced, merely displayed as amorphous phases, but incidentally ordering could still occur, albeit non-detectable for WAXD (see Figure 4b).

Another aspect was the apparent transparency of the 24/76% of cellulose-xylan stretched film, although it was completely non-transparent in a non-stretched fashion. Non-transparency indicates phase separation due to xylan self-assembly out of the surrounding cellulose matrix. The re-ordering behavior was similar to polyethylene (Chanzy et al. 1987) except that recrystallization did not occur after the drying process. Polarized microscopic images of this specific stretched gel did not exhibit any birefringence, and therefore, it could be safely concluded that stretching was capable of disrupting the earlier formed crystallites in an easy way.

Considering the native aspects of the plant cell wall, in which the composition of cellulose-glucuronoxylan is well represented by 65/35% and cellulose-xyloglucan by 60/40%, it was clear that the interaction between cellulose and xyloglucan is stronger than the interaction between cellulose and glucuronoxylan. This can possibly be explained by the relatively weak interference of the xylose substituents on the C-6 position of the xyloglucan in comparison to the steric hindrance of the 4-O-methyl glucuronic acid group. Although in the native system lignin is far away located from the interaction between cellulose and xylan, a small contamination of lignin could occur in the glucuronoxylan, bound to the xylan backbone chain via an ether linkage, and although a small amount, it could trigger the aggregation of xylan molecules (Roubroeks et al. 2004).

### Surface characteristics of stretched cellulose-hemicellulose blended films

Stretched dried films of the cellulose-xyloglucan and cellulose-xylan were investigated in order to determine the surface characteristics as a reflection of the interaction between the two polymer systems. Most of the surface characteristics were determined at the micrometer scale. The different phases in a polymer matrix were identified with DFM, which worked in tapping mode as shown in Figure 5. This analytical technique confirmed the results of WAXD in the

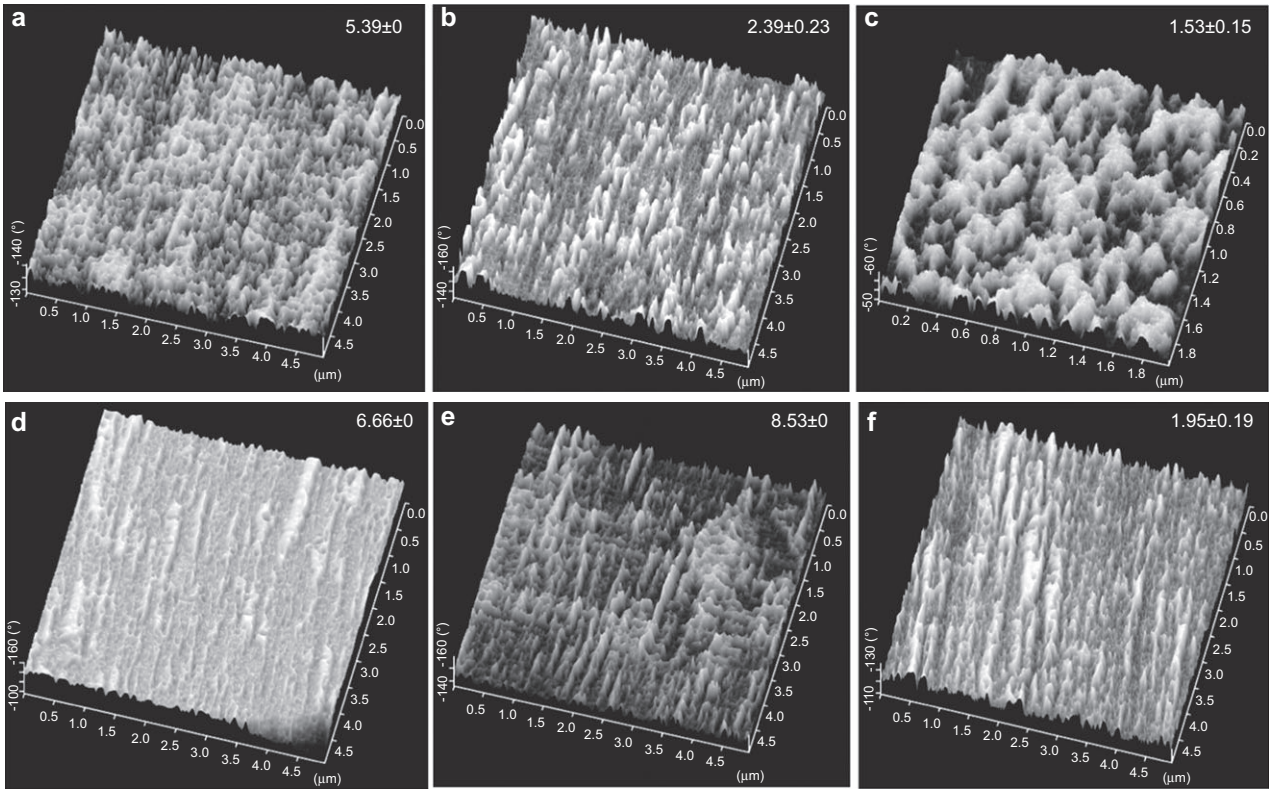


**Figure 5** DFM of the surface on the blended films of (a) 85/15% cellulose-xylan, (b) 65/35% cellulose-xylan, (c) 24/76% cellulose-xylan (d) 80/20% cellulose-xyloglucan, (e) 70/30% cellulose-xyloglucan, (f) 60/40% cellulose-xyloglucan phase image. RMS (root mean square) values are in nm.

previous section. At a micrometer scale in an area of 5×5 $\mu m^2$, the orientation and the polymer phases could be evaluated in the phase images. In general, the interaction mode, presented by the dynamic force between the cantilever and the surface morphology, is visualized by the software as dark regions indicating "hard" regions (crystalline or semicrystalline), while brighter regions were "soft" (non-crystalline regions). Figure 5a–c shows DFM images with increasing xylan concentration from 85/15% to 24/76% of cellulose-xylan. The orientation and regularity of the surface in 85/15% (a) could be clearly observed, while 65/35% (b) indicated a larger distribution of "soft" regions on the surface, but maintaining orientation. Nevertheless, it simultaneously indicates the initiation of the phase separation of xylan from the cellulose matrix. The image of Figure 5c exhibits non-order and non-crystalline (amorphous) structures, present on the surface of 24/76% cellulose-xylan with more "soft" than "hard" regions. The root mean square (RMS) values in the figures show the homogeneity of the surface property. A small RMS value is indicative of a homogeneous surface property. The RMS values of (a) and (b) decreased with an increasing xylan content, which indicates more homogeneity. Figure 5c (24/76%) of cellulose-xylan illustrates a random orientation with the lowest RMS value (1.53±0.15 nm), which is a representative for homogeneously distributed "soft" regions that were in an amorphous state. However, this sample cannot be interpreted as being the best composition; it has been clearly demonstrated by WAXD and microscopic FTIR that xylan molecules phase separate out of the surrounding cellulose matrix. The discontinuity between the WAXD and DFM experiments indicate that amorphous domains cover the surface, but semicrystalline phase-separated domains of xylan are distributed inside the film at compositions containing more than 30% of xylan.

Blends of cellulose-xyloglucan clearly showed a more regular orientation at compositions ranging from 80/20% until 60/40% (Figure 5d–f). High RMS values for samples (d) and (e) reveal more heterogeneity on the surface properties, although orientation is present. A further increase of the xyloglucan concentration results in lower RMS values, indicating that cellulose-xyloglucan 60/40% has the highest compatibility and feasibility for good interactions. It is likely that the most similar composition to the native primary cell wall system can be close to 60/40% cellulose-xyloglucan.

A direct measurement of the surface characteristics of the cellulose-xylan and cellulose-xyloglucan blended films could be obtained by contact angle (CA) determination. By means of the CA technique, a relationship of the surface characteristics and the polymer composition could be obtained. The results of the combined experiments with xylan and xyloglucan are presented in Figure 6. The NOC sample was used as a reference, and the CA value was ca. 70° (Kondo et al. 2001). A 5% increase in xylan composition resulted in a more hydrophobic surface. The addition of more xylan, however, led to a gradual decrease of the hydrophobicity. This could be attributed to changes in molecular chain (glucopyranose planes) tilting with respect to the initial tilting angle of ca. 30°

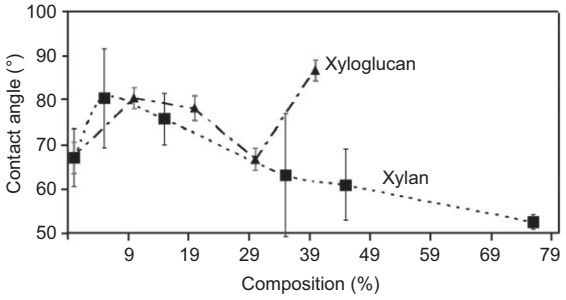


**Figure 6** Relationship between the xylan or xyloglucan composition of the blend and the surface property [contact angle (°)].

in NOC (Kondo 2007). Xyloglucan displays a very similar behavior; the first increase of the surface hydrophobicity is followed by a gradual decrease with elevated content of the xyloglucan component until 30%. However, the composition 60/40% exhibited a drastic change in surface hydrophobicity in comparison to other compositions as well as NOC. It remains unclear whether this observation is also related to the tilting of the molecular chains.

Addition of either xyloglucan or xylan to cellulose resulted in the formation of homogeneously distributed "soft" regions on the surface at compositions over 30% in favor of the hemicelluloses. The difference between xylan and xyloglucan at compositions more than 35% appeared in the surface structure; namely, the oriented surface structure was present in xyloglucan, whereas no such surface structure occurred with xylan. This result clearly shows the importance of oriented surface structures in native systems.

## Conclusion

Blends of cellulose and xylan/ or xyloglucan were prepared by molecular mixing. The coagulated, non-stretched water-swollen cellulose-xylan (>50% of xylan) gel-like films were not transparent, indicating a semicrystalline behavior of the xylan phase as also confirmed by X-ray diffraction after complete drying. Namely, it appeared that a phase separation due to xylan self-assembly out of the surrounding cellulose matrix occurred. Under crossed-Nicols of a polarized microscope, it could be observed that negative-type spherulites formed with an average diameter of 38 μm. Uniaxial stretching of the water-swollen films of cellulose-xylan 24/76% resulted in disrupting these crystallites. Stretching rendered a non-ordered, amorphous gel as observed by WAXD.

Non-stretched dried cellulose-xyloglucan blended films were completely transparent, indicating a completely non-crystalline state. Stretched films of blends with xyloglucan followed the NOC pattern. This indicates the possibility for a tight interaction between cellulose and xyloglucan.

The surface analysis at a micrometer scale with DFM indicated that at concentrations higher than 35% of xylan, more homogeneously distributed "soft" regions occurred but in an amorphous state. This resulted in an increase of the

surface hydrophilicity. In the case of xyloglucan, a decrease in RMS value could be observed, which was accompanied with increasing xyloglucan compositions, i.e., homogeneity and order was increasing. At compositions higher than 35% of xylan or xyloglucan, changes in the surface property could be measured, which clearly shows the importance of ordered structures. These results are in relation to open questions regarding the matrix of the plant cell wall. The inclusion of hemicellulose components and the molecular interaction between cellulose and hemicelluloses in stretched conditions reveals an effect on the mechanism of cellulose ordering. Moreover, with regard to the optimal compositions between the biocomponents, it was observed that phase separation of xylan out of the surrounding cellulose matrix started to occur at compositions above 35% of xylan being close to the relative composition found in the native secondary plant cell wall. The matrix between cellulose and xyloglucan indicated that the lowest RMS value was observed for the composition 60/40% of cellulose-xyloglucan. This composition shows excellent compatibility and feasibility of a tight interaction and therefore probably being close to the native composition in the primary cell wall matrix.

## Acknowledgments

The authors wish to thank Drs. W. Kasai and Y. Tomita at the Graduate School of Bioresource and Bioenvironmental Sciences, Kyushu University, Japan for their valuable help on the microscopic observations. Mr. E. Togawa from Forestry and Forest Products Research Institute (FFPRI), Tsukuba, Japan is greatly thanked for all the help in preparation and running WAXD experiments. This research was partly supported by a Grant-in-Aid for Scientific Research (No. 22380097), Japan Society for the Promotion of Science (JSPS).

## References

Abe, H., Funada, R., Ohtani, J., Fukazawa, K. (1995) Changes in the arrangement of microtubules and microfibrils in differentiating conifer tracheids during expansion of cells. Ann. Bot. 75:305–310.

Abe, H., Funada, R., Ohtani, J., Fukazawa, K. (1997) Changes in the arrangement of cellulose microfibrils associated with the cessation of cell expansion in tracheids. Trees 11:328–332.

Åkerholm, M., Salmén, L. (2001) Interactions between wood polymers studied by dynamic FT-IR spectroscopy. Polymer 42: 963–969.

Atalla, R.H., Hackney, J.M., Uhlin, I., Thompson, N.S. (1993) Hemicelluloses as structure regulators in the aggregation of native cellulose. Int. J. Biol. Macromol. 15:109–112.

Bootten, T.J., Harris, P.J., Melton, L.D., Newman, R.H. (2009) Solid-state 13C NMR study of a composite of tobacco xyloglucan and *Gluconacetobacter xylinus* cellulose: molecular interactions between the component polysaccharides. Biomacromolecules 10:2961–2967.

Carpita, N., McCann, M. (2000) Biochemistry and Molecular Biology of Plants. Eds. Buchanan, B., Gruissem, W., Jones, R. American Society of Plant Physiologists, Rockville, Maryland. pp. 52–108.

Chanzy, H., Smith, P., Revol, J.-F., Manley, R. St. J. (1987) High-resolution electron microscopy of ultradrawn gels of high molecular weight polyethylene. Polymer Comm. 28:133–136.

Cosgrove, D.J. (2001) Wall structure and wall loosening. A look backwards and forwards. Plant Physiol. 125:131–134.

Ebringerová, A., Heinze, T. (1999) Xylan and xylan derivatives – biopolymers with valuable properties, 1. Naturally occurring xylans structures, isolation procedures and properties. Macromol. Rapid Comm. 21:542–556.

Finkenstadt, V.L., Hendrixson, T.L., Millane, R.P. (1995) Models of xyloglucan binding to cellulose microfibrils. J. Carbohydr. Chem. 14:601–611.

Hanus, J., Mazeau, K. (2006) The xyloglucan-cellulose assembly at the atomic scale. Biopolymers 82:59–73.

Hayashi, T. (1989) Xyloglucans in the primary wall. Ann. Rev. Plant Physiol. Plant Mol. Biol. 40:139–168.

Hayashi, T., MacLachlan, G. (1984) Pea xyloglucan and cellulose. I. Macromolecular organisation. Plant Physiol. 75:596–604.

Hayashi, T., Ogawa, K., Mitsuishi, Y. (1994) Characterization of the adsorption of xyloglucan to cellulose. Plant Cell Physiol. 35:1199–1205.

Iwata, T., Indrarti, L., Azuma, J. (1998) Affinity of hemicellulose for cellulose produced by *Acetobacter xylinum*. Cellulose 5:215–228.

Jacobs, A., Larsson, P.T., Dahlman, O. (2001) Distribution of uronic acids in xylans from various species of soft- and hardwood as determined by MALDI mass spectrometry. Biomacromolecules 2:979–990.

Kataoka, Y., Kondo, T. (1999) Quantitative analysis for the cellulose Iα crystalline phase in developing wood cell walls. Int. J. Biol. Macromol. 24:37–41.

Kondo, T. 2007. Nematic ordered cellulose: its structure and properties. In: Cellulose: Molecular and Structural Biology. Eds. Brown, Jr. R.M., Saxena, I.M. Springer, Dordrecht, The Netherlands. pp. 285–306.

Kondo, T., Togawa, E., Brown Jr., R.M. (2001) Nematic ordered cellulose: a concept of glucan-chain association. Biomacromolecules 2:1324–1330.

Kroon-Batenburg, L.M.J., Kroon, J., Leeflang, B.R., Vliegenthart, J.F.G. (1993) Conformational analysis of methyl β-cellobioside by ROESY NMR spectroscopy and MD simulations in combination with the CROSREL method. Carbohydr. Res. 245:21–42.

Levy, S., York, W.S., Stuike-Prill, R., Meyer, B., Staehelin, L.A. (1991) Simulations of the static and dynamic molecular conformation of xyloglucan. The role of the fucosylated sidechain in surface-specific sidechain folding. Plant J. 1:195–215.

Mandelkern, L. (1964) Morphology. In: Crystallisation of Polymers, McGraw-Hill Book company, New York.

Marchessault, R.H., Settineri, W.J. (1964) Some comments on the crystallography of xylan hydrate. Polym. Lett. 2:1047–1051.

McCann, M.C., Wells, B., Roberts, K. (1990) Direct visualization of cross-links in the primary plant cell wall. J. Cell Sci. 96:323–334.

Neville, A.C. (1988) A pipe-cleaner molecular model for morphogenesis of helicoidal plant cell walls based on hemicellulose complexity. J. Theor. Biol. 131:243–254.

Reis, D., Vian, B., Roland, J.-C. (1994) Cellulose-glucuronoxylans and plant cell wall structure. Micron. 25:171–187.

Roubroeks, J.P., Saake, B., Glasser, W.G., Gatenholm, P. (2004) Contribution of the molecular architecture of 4-O-methyl glucuronoxylan to its aggregation behaviour in solution. In: Hemicelluloses Science and Technology. Eds, Gatenholm, P., Tenkanen, M. ACS Symp. Ser. 864:167–183.

Salmén, L. Burgert, I. (2009) Cell wall features with regard to mechanical performance. A review. COST Action E35 2004–2008: wood machining – micromechanics and fracture. Holzforschung 63:121–129.

Stevanic, J.S., Salmén, L. (2009) Orientation of the wood polymers in the cell wall of spruce wood fibres. Holzforschung 63:497–503.

Sugiyama, J., Persson, J., Chanzy, H. (1991) Combined infrared and electron diffraction study of the polymorphism of native celluloses. Macromolecules 24:2461–2466.

Uhlin, K.I., Atalla, R.H., Thompson, N.S. (1995) Influence of hemicelluloses on the aggregation patterns of bacterial cellulose. Cellulose 2:129–144.

Vian, B., Reis, D., Mosiniak, M., Roland, J.-C. (1986) The glucuronoxylans and the helicoidal shift in cellulose microfibrils in linden wood: cytochemistry *in muro* and on isolated molecules. Protoplasma 131:185–189.

Whitney, S.E.C., Brigham, J.E. Darke, A.H., Reid, J.S.G., Gidley, M.J. (1995) *In vitro* assembly of cellulose/xyloglucan networks: ultrastructural and molecular aspects. Plant J. 8: 491–504.

Whitney, S.E.C., Brigham, J.E., Darke, A.H., Reid, J.S.G., Gidley, M.J. (1998) Structural aspects of the interaction of mannan-based polysaccharides with bacterial cellulose. Carbohydr. Res. 307:299–309.

Received July 6, 2011. Accepted May 25, 2012. Previously published online June 22, 2012.